Ultrafast, temporally stochastic STED nanoscopy of millisecond dynamics

Jale Schneider[1,2], Jasmin Zahn[1,2], Marta Maglione[3], Stephan J Sigrist[3], Jonas Marquard[1,2], Jakub Chojnacki[4], Hans-Georg Kräusslich[4], Steffen J Sahl[5], Johann Engelhardt[1,2] & Stefan W Hell[1,2,5]

Electro-optical scanning (>1,000 frames/s) with pixel dwell times on the order of the lifetime of the fluorescent molecular state renders stimulated emission depletion (STED) nanoscopy temporally stochastic. Photon detection from a molecule occurs stochastically in one of several scanning frames, and the spatial origin of the photon is known with subdiffraction precision. Images are built up by binning consecutive frames, making the time resolution freely adjustable. We demonstrated nanoscopy of vesicle motions in living *Drosophila* larvae and the cellular uptake of viral particles with 5- to 10-ms temporal resolution.

Super-resolution fluorescence microscopes, also known as nanoscopes, discern fluorophores located within subdiffraction distances by ensuring that the fluorophores to be separated are in two different states when illuminated by the same diffraction excitation pattern[1]. Usually these states are 'on' and 'off' states of fluorescence emission, as on versus off provides good separation contrast[1]. There are two ways of inducing a spatial difference in molecular states in the sample: coordinate targeted and coordinate stochastic. The first approach, realized in methods such as STED, saturated structured illumination and reversible saturable/switchable optically linear fluorescence transitions (RESOLFT), employs a pattern of light featuring one or more intensity minima, transferring all fluorophores to one of these states except those located at the minima. The location of the specific states and hence of the emitting molecules is thus firmly determined by the illumination pattern, which is then scanned to examine all fluorophores in the sample. In contrast, the spatially stochastic methods, such as photoactivated localization microscopy (PALM)[2,3] and stochastic optical reconstruction microscopy (STORM)[4], induce the state difference randomly in space by installing the on state molecule by molecule. The position of the on-state molecule is then determined by localization, using the emitted light pattern.

Stochasticity in space must not be confused with stochasticity in time. For example, the state transfer and localization of single molecules can be spatially stochastic but still temporally controlled. In fact, initial realizations of PALM/STORM used sequences of light pulses dedicated to the off-on transfer (activation), fluorescence generation and the on-off transition (bleaching), each arriving at controlled time points at the sample. Apart from the method termed points accumulation for imaging in nanoscale topography (PAINT), which produces images during the temporally stochastic binding of diffusing fluorescent molecules[5], temporal randomness was originally realized in the method called PALMIRA (PALM with independently running acquisition)[6], in which all the above processes were performed with a single continuous-wave (CW) beam and fluorescence was recorded with a freely running camera. Thus, the time points of the molecular state transfers and localizations were totally random. Meanwhile, temporal stochasticity is taken for granted as a feature of modern PALM/STORM and related methods (for example, in the dark-state switching of fluorescent proteins or common dyes[7,8]) because it has provided technical simplicity and increased recording speed.

However, because spatial and temporal stochasticity are distinct matters, this reasoning brings up the question as to whether it is possible to realize a coordinate-targeted super-resolution method, i.e., one that is spatially deterministic, in a temporally stochastic fashion. Here, we present a STED[9] nanoscope that comes close to this ideal owing to the introduction of ultrafast electro-optical scanning. The scanning speed is so fast that the pixel dwell times reach the fundamental limit of the lifetime of the fluorescent state. With imaging of >1,000 frames per second (f.p.s.), data acquisition is pushed to a regime where the image becomes assembled 'one photon at a time', in a temporally stochastic manner. This STED modality has the obvious potential to detect dynamic processes at higher imaging rates and provides increased photon yield—here it was up to fivefold higher—in standard fluorophores compared to slow scanning.

Sufficient temporal resolution is essential to avoid spatial information loss, which is why several techniques have been developed to increase imaging speed[10–13]. Standard laser scanning microscopy is limited in this regard because the inertia of the galvanometer-driven mirrors employed for beam deflection restricts the attainable line frequency to a few kilohertz. The line frequency can be raised up to 20 kHz by driving the mirrors in resonance, even for large fields[14], but this approach has its own limitations[11]. Acousto-optical deflectors allow line rates up to a few hundred kilohertz[15], but wavelength-dependent deflection angles and beam distortions render the system complex[16–18].

[1]German Cancer Research Center (DKFZ), Optical Nanoscopy Division, Heidelberg, Germany. [2]Bioquant Center, Heidelberg, Germany. [3]Institute for Biology and Genetics, Free University of Berlin, Berlin, Germany. [4]Department of Infectious Diseases, Virology, University of Heidelberg, Heidelberg, Germany. [5]Department of NanoBiophotonics, Max Planck Institute for Biophysical Chemistry, Göttingen, Germany. Correspondence should be addressed to S.W.H. (shell@mpibpc.mpg.de).

RECEIVED 31 JANUARY; ACCEPTED 11 JUNE; PUBLISHED ONLINE 27 JULY 2015; DOI:10.1038/NMETH.3481

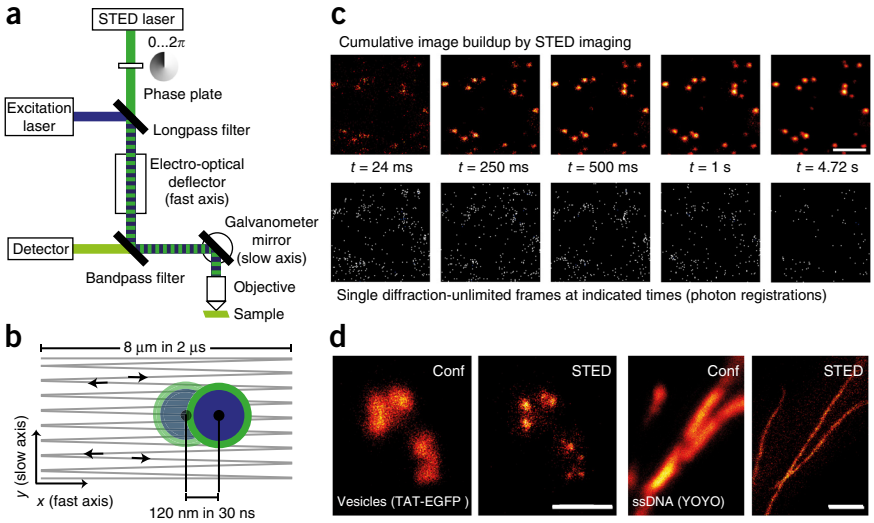

Figure 1 | Ultrafast STED scanning and temporally stochastic image assembly. (**a**) The setup: the electro-optical deflector scans the fast axis at a line frequency of 250 kHz; the galvanometer mirrors scan the slow axis. (**b**) STED scan pattern. The blue circle represents the excitation light spot. The inner black circle is the region where the fluorescent state remains allowed (with common center given by the intensity minimum of the STED doughnut, which is schematically represented as the green overlaid circle). A fluorophore typically undergoes numerous excitation-emission (and, in STED, de-excitation) cycles in succession, until the beam or beams completely leave the area. For ultrafast scanning, the number of subsequent pulses per diffraction-limited region decreases drastically. (**c**) Cumulative buildup (top row) of super-resolution image of HIV labeled with EGFP by addition of single STED frames (bottom row, here acquired at 416 Hz). Virus particles can be identified in <250 ms, and acquisition can be stopped as soon as the signal is sufficient or bleaching becomes dominant. (**d**) Confocal and STED images of endocytotic vesicles labeled with TAT-EGFP (left), and ssDNA labeled with YOYO (right). Images are representative of >20 data sets of similar quality. Scale bars, 1 µm.

The use of an electro-optical deflector (EOD) reported herein allows the realization of what is to the best of our knowledge the fastest laser scanning microscope to date (**Fig. 1a**). An EOD deflects beams of any wavelength in proportion to the high-voltage field applied over its entire cross-section. Displaying no inertia, the crystal responds within a few hundred picoseconds. Therefore, in our system (**Fig. 1b**), the fast axis is scanned by an EOD providing a line frequency of 250 kHz. The slow axis is served by galvanometer mirrors, thus yielding rates of ~1,000 f.p.s. when sampling 250 × 320 pixels.

In confocal microscopes with approximately microsecond pixel dwell times, fluorophores typically face 10–1,000 excitation events until the illumination spot is moved, usually after a certain number of photons are collected on average. Thus, the excitation, detection and bleaching events appear continuous despite the stochastic nature of these processes. Only if the dwell time of the moving illumination spot on a fluorophore is shorter than the average pause between two excitation events will the molecule not be subjected to multiple events. In this case, the molecule will emit at most one photon per illumination cycle, preserving the stochastic nature of the emission from the interrogated pixel. In the simple but common situation of excitation with relatively bright pulses that are shorter than the fluorescent state lifetime, the light exposure of a molecule typically must be shorter than the interval between two pulses.

Delivering a line-scanning frequency of 250 kHz (**Fig. 1a**,**b**), the EOD[19] kept the number of consecutive excitation pulses per diffraction-sized region (per scan cycle) down to one or two pulses in one-dimensional (1D) and 8–10 pulses in 2D scanning. The stochastic nature of the fluorophore-light interaction is thus conserved, producing randomness in the timing of emission events over the course of multiple frame cycles. Yet, the spatial origin of every photon emission is defined as precisely and accurately as in any other coordinate-targeted (STED) nanoscopy because it is dictated by the fluorescence-inhibiting STED beam. Note that definitions of pixel sizes and dwell times become coupled to the fluorescence lifetime, as they are freely definable and no longer dependent on technical factors. Pixel dwell times are as short as the fluorescence lifetime, and the pixel size is simply the distance scanned within the lifetime period.

In our implementation (Online Methods), scan fields reached up to 8 µm for a 100× magnifying objective lens, or up to 12 µm for 63× lenses, depending on the voltage. The pixel dwell time was chosen to be 6.25 ns to cover the lifetime of most fluorophores. Shorter pixel dwell times could also be realized. The line-scan duration was 2 µs, giving 320 pixels on the fast axis. The pixel size was varied by the voltage and by the magnification factor. Compared to galvanometer scanning in both axes, the scan speed was raised from a few nanometers to 4 µm per microsecond. Therefore, depending on the pulse repetition rate, subsequent laser pulses addressed different pixels that could be further apart than the size of the diffraction-limited light spot. **Table 1** compares our ultrafast with conventional scan modalities for the present configuration using a 100× lens and a 30-MHz laser pulse repetition rate (Online Methods).

During image acquisition, single full frames acquired within ~1 ms were continuously added on-line. Such cumulative image construction appears reminiscent of spatially (and temporally) stochastic super-resolution techniques such as PALMIRA[6] and most of the other spatially stochastic techniques, but in a fashion that is coordinate controlled (**Fig. 1c**). The ultrahigh frame rate enables dynamic adjustment of data acquisition time and of light dose, which can be changed from frame to frame. In many cases, a few photons are sufficient to create contrast and identify

Table 1 | Comparison of the number of laser pulses

	Conventional scan (line frequency of 1 kHz)	Ultrafast scan (line frequency of 250 kHz)
Number of pulses per diffraction-limited region in 1D scanning	325	1.3
Number of pulses per diffraction-limited region in 2D scanning	2,325	9.3
Number of frames to be captured	1	250
Sum of pulses	2,325	2,325

Values were obtained using a 100× objective and a laser repetition rate of 30 MHz.

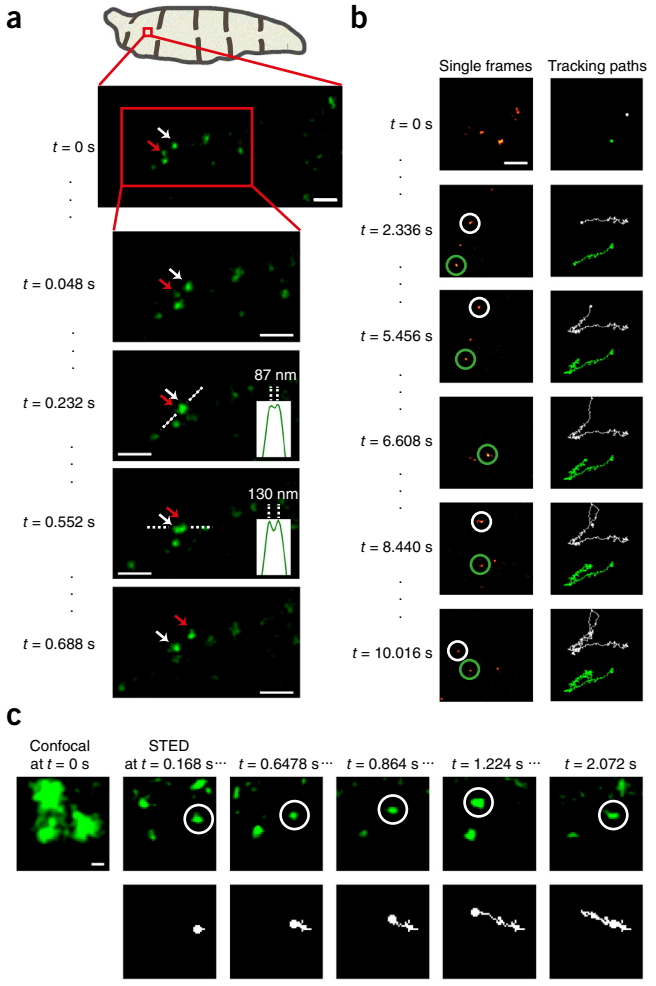

Figure 2 | STED imaging of millisecond-scale dynamic processes. (**a**) Live STED imaging of EGFP-labeled vesicles in neuron of *Drosophila* larvae with a temporal resolution of 8 ms (125 f.p.s.). The red arrows point out one fast-moving vesicle with a speed of up to 1.8 µm/s overtaking another moving vesicle pointed out by the white arrows. Scale bars, 1 µm. (**b**) Live STED imaging of cellular uptake of vesicular stomatitis virus glycoprotein G (VSV-G)-pseudotyped EGFP-labeled HIV-1 particles at a temporal resolution of 8 ms (see also **Supplementary Video 5**). The left panels show single frames with a spatial Gaussian filtering of 100-nm width. The tracking paths of two manually tracked virus particles are shown in the right panels. Scale bar, 1 µm. (**c**) Zoomed-in view of another example of imaging in *Drosophila* larvae highlighting the resolution improvement by STED. The effective frame rate is 125 f.p.s. as in **a**. The data are spatially filtered with a Gaussian of 50-nm width; they are temporally filtered with a moving window filter with a window size over ten frames and window shift over three frames. Scale bar, 200 nm. Images are representative of >20 (*Drosophila*) and ~5 (viral uptake) data sets of similar quality.

structures of interest, with images constructed within a second or two. For example, after just 0.25 s, single EGFP-labeled HIV particles were resolved (**Fig. 1c** and **Supplementary Video 1**). Longer accumulation of frames increases signal but also the total light dose. Other images of dimly labeled structures are shown in **Figure 1d**. The imaging of (fixed) samples may be halted as soon as the required signal is reached because the image is built up by fast addition of frames.

Bleaching originating from the first excited (singlet) state poses problems in all fluorescence applications, including STED. Nonetheless, it is worth appreciating that stimulated emission *per se* efficiently transfers molecules out of the excited state to the non-reactive ground state. STED beam–induced bleaching occurs because the photons of this beam can also effect transitions to higher-lying reactive states, such as triplet states and their progenies[20–22]. Because of the minimal number of laser pulses per molecule per scan cycle in our approach, only a few fluorophore molecules are encountered in the triplet state. Within the pauses between two lines and within the longer pauses frame to frame, most fluorophores can relax from the triplet or dark state to the ground state[23]. Therefore, our fast scanning approach reduces bleaching and blinking. In fact, we compared the fluorescence yield of new ultrafast scanning with that of conventional (slow) scanning by imaging equally sized and dense areas for equal durations. For many fluorophores and laser configurations, we observed that the total signal increased by 1.5- to 4.5-fold when ultrafast scanning was used (**Supplementary Fig. 1**).

A geometrical effect additionally improves the images. In single-beam-scanning STED imaging (**Fig. 1b**), a fluorophore normally undergoes many excitation and de-excitation cycles before it encounters the position of the minimum of the STED (doughnut) beam, where it can fluoresce. In slow scanning, fluorophores may thus undergo thousands of excitation and de-excitation cycles and bleach before contributing fluorescence. In ultrafast scanning, owing to the quasi temporally random nature of the light-molecule interaction, the de-excitation and the (spontaneous) fluorescence transitions are almost evenly distributed over time. Consequently, the likelihood of extracting signal before bleaching is increased. In our setup, samples labeled with EGFP were excited with 5- to 10-µW average power at the back pupil plane of the lens (5–10 kW/cm^2). The corresponding STED laser power was 20–50 mW (~20–50 MW/cm^2, ~2–6 nJ per pulse).

Pixel dwell times on the order of the fluorescence lifetime allowed the observation of dynamic processes with freely adjustable temporal resolution (as multiples of the ~1-ms frame time). Single frames could be buffered and binned on-line or off-line, depending on the movement of the features observed. Data filters, such as a median filter, could be chosen accordingly. Features with high labeling density could be captured at up to 1,000 f.p.s. on 250 × 320 pixels (**Supplementary Video 2**). Smaller image fields would result in even higher frame rates.

In general, the recording speed depends on only the fluorescence signal strength. We recorded STED videos at >100 f.p.s. (after on-line binning) in EGFP-labeled living samples. An *in vivo* observation of vesicle trafficking along motor neurons in *Drosophila* larvae is shown in **Figure 2a**,**c** (see also **Supplementary Videos 3** and **4**). Vesicles moving at 1.8 µm/s necessitated frame rates of ≥72 f.p.s., otherwise the assignment of detected photons to individual pixels would have been incorrect (owing to motion blur). This example highlights the importance of recording at maximum speed and producing the super-resolution movie at the maximum frame rate supported by the signal. We then performed another, dynamic study of HIV in living cells (**Fig. 2b** and **Supplementary Video 5**). Virus speeds up to 2 µm/s required a frame rate of ≥85 f.p.s. The pixel size was set to 25 nm and the effective frame rate to 125 f.p.s. (on-line binning), for a resolution of ~70 nm.

In conclusion, electro-optical scanning has enabled the fastest nanoscopy to date. Flexible binning of frames recorded with pixel

dwell times at the fluorescence lifetime limit allows the effective frame rate to be adapted to the dynamic process under investigation, notably also after recording. At its core, the achieved recording speed is by virtue of the coordinate-targeted nature of our super-resolution method: the position of the emitter is known at all times because it is determined by the many photons of the STED beam. The resolution itself is not negatively affected by ultrafast scanning; on the contrary, the decreased bleaching typically provides higher resolution (**Supplementary Figs. 2** and **3**), even for the dimmest objects. Finally, we note that current limits of the field of view can be overcome by implementing multispot approaches with no negative impact on frame rate.

METHODS

Methods and any associated references are available in the online version of the paper.

Note: Any Supplementary Information and Source Data files are available in the online version of the paper.

ACKNOWLEDGMENTS

We thank D. Richardson (MPI-BPC, now at Harvard University) and C. Gregor (MPI-BPC) for providing the TAT-EGFP samples, as well as H. Ta for advice on single-emitter STED measurements. We thank T. Hope (University of Illinois) for the plasmid pEGFP.Vpr. This work was supported by a Leibniz Award of the Deutsche Forschungsgemeinschaft (to S.W.H.) and by the German Federal Ministry of Education and Research (BMBF) within the project STEDlight (FKZ: 13N11173).

AUTHOR CONTRIBUTIONS

J.S. and J.E. developed the EOD scanning system and set up the microscope. J.S. and J.Z. performed the experiments and analyzed the data. M.M., S.J. Sigrist, J.C. and H.-G.K. provided samples. J.M. performed single-antibody imaging. J.S., J.E., S.J. Sahl and S.W.H. wrote the manuscript. The latter also conceived and guided the project and is responsible for its main points. All authors discussed the data and commented on the manuscript.

COMPETING FINANCIAL INTERESTS

The authors declare no competing financial interests.

1. Hell, S.W. *Science* **316**, 1153–1158 (2007).
2. Betzig, E. *et al. Science* **313**, 1642–1645 (2006).
3. Hess, S.T., Girirajan, T.P.K. & Mason, M.D. *Biophys. J.* **91**, 4258–4272 (2006).
4. Rust, M.J., Bates, M. & Zhuang, X.W. *Nat. Methods* **3**, 793–795 (2006).
5. Sharonov, A. & Hochstrasser, R.M. *Proc. Natl. Acad. Sci. USA* **103**, 18911–18916 (2006).
6. Egner, A. *et al. Biophys. J.* **93**, 3285–3290 (2007).
7. Biteen, J.S. *et al. Nat. Methods* **5**, 947–949 (2008).
8. Fölling, J. *et al. Nat. Methods* **5**, 943–945 (2008).
9. Hell, S.W. & Wichmann, J. *Opt. Lett.* **19**, 780–782 (1994).
10. Tsien, R.Y. & Backsai, B.J. in *Handbook of Biological Confocal Microscopy* 2nd edn. (ed. Pawley, J.) 459–478 (Plenum Press, New York, 1996).
11. Westphal, V. *et al. Science* **320**, 246–249 (2008).
12. Huang, F. *et al. Nat. Methods* **10**, 653–658 (2013).
13. Lauterbach, M.A., Ullal, C.K., Westphal, V. & Hell, S.W. *Langmuir* **26**, 14400–14404 (2010).
14. Wu, X., Toro, L., Stefani, E. & Wu, Y. *J. Microsc.* **257**, 31–38 (2015).
15. Rietdorf, J. & Stelzer, E.H.K. in *Handbook of Biological Confocal Microscopy* 3rd edn. (ed. Pawley, J.) Ch. 3, 43–58 (Springer, New York, 2006).
16. Chen, X., Leischner, U., Rochefort, N.L., Nelken, I. & Konnerth, A. *Nature* **475**, 501–505 (2011).
17. Kremer, Y. *et al. Opt. Express* **16**, 10066–10076 (2008).
18. Salomé, R. *et al. J. Neurosci. Methods* **154**, 161–174 (2006).
19. Engelhardt, J., Özcelik, J. & Hell, S.W. Elektrooptische Anordnung zum ultraschnellen Abtasten eines Objektes. German patent DE 202010004547 U1 (2011) and European patent application WO2012171999 A1 (2012).
20. Diaspro, A., Chirico, G., Usai, C., Ramoino, P. & Dobrucki, J. in *Handbook of Biological Confocal Microscopy* 3rd edn. (ed. Pawley, J.) Ch. 39, 690–700 (Springer, New York, 2006).
21. Eggeling, C., Widengren, J., Rigler, R. & Seidel, C.A.M. *Anal. Chem.* **70**, 2651–2659 (1998).
22. Tsien, R.Y., Ernst, L. & Waggoner, A. in *Handbook of Biological Confocal Microscopy* 3rd edn. (ed. Pawley, J.) Ch. 16, 338–352 (Springer, New York, 2006).
23. Donnert, G., Eggeling, C. & Hell, S.W. *Nat. Methods* **4**, 81–86 (2007).

ONLINE METHODS

Optical setup. The setup employs a pulsed (31.512 MHz) Raman fiber laser (PRFL Series, MPB Communication Inc.) operating at 560 nm for stimulated emission and a pulsed diode laser operating at 485 nm (LDH-P-C-485 PicoQuant GmbH) for excitation. The STED beam passes through a phase plate (VPP-2, RPC Photonics), which induces a spatially varying phase delay resulting in a doughnut-shaped intensity profile at the lens focal plane. The excitation and STED beams are spatially overlaid by a longpass filter (BLP01-561, Semrock Inc.). A delay box facilitates the temporal overlay of both pulse trains, with the STED laser triggering the diode laser. The beams travel together through the electro-optical deflector (M311A, Conoptics Inc.), which scans the fast axis. Two galvanometer mirrors (6210H, Cambridge Technologies), as part of a 'quad-scanner' arrangement[24], scan the slow axis. Although only one galvanometer per axis is in principle sufficient, the use of two per axis allows more flexibility to change the lateral position as well as the beam pivot point in the pupil. The beams are focused on the sample by an oil objective (100×, 1.4 NA, HCX PL APO, Leica Microsystems). A bandpass filter (ET525/50M, Chroma Technology Corp.) separates the fluorescence emission from the STED and excitation lasers at an angle of incidence of ~15°. The fluorescence signal is de-scanned by the galvanometer mirrors but not by the electro-optical deflector owing to its polarization-dependent transmission. Therefore, a slit instead of a pinhole is placed in front of the hybrid photodetector (R10467U-40 Hamamatsu). The detector has a large sensitive area of 1 mm^2 and is placed into the pupil plane. A further bandpass filter (FF03-525/50, Semrock Inc.) additionally suppresses the residual laser light. Note that when a pinhole is employed, the intensity contribution at the detector from out-of-focus light essentially decreases with $\sim 1/r^2$, and with $\sim 1/r$ in the case of a slit (where r is the distance from the focal plane). So there is out-of-focus light suppression by the confocal slit, but it scales less favorably. However, because the STED doughnut also suppresses fluorescence emission, this weakness is partially compensated. The electro-optical deflector operates at a deflection angle up to ±7.2 mrad, which translates into a line width of up to 8 µm in the image plane. The pixel clock is chosen as 160 MHz, resulting in a pixel dwell time of 6.25 ns and 320 pixels for the fast axis. The number of lines on the slow axis can be chosen flexibly. An FPGA-based data-processing unit samples the fluorescence signal, controls and synchronizes the scanner and constructs the image, assigning photons to pixels. The synchronization output of the signal-generator card controlling the fast scanner serves as master clock running at the line frequency of 250 kHz. A timed loop running at 160 MHz within the FPGA program acts as pixel clock. This loop also samples the master clock, to set the pixel number to 0 on each line start and to trigger the voltage increases on the galvanometer mirrors. Consequently, for every cycle of the loop, the x-y coordinates of the laser in the sample plane are known. The identical loop samples the detector signal, so it can assign the coordinate to each detected photon. The pixel clock and clock signal of the pulsed laser source run asynchronously. Whereas in a normal scanning system one can always predict a narrow time interval (given by the time point of the scanning beam arriving at a given pixel coordinate and the ~µs pixel dwell time) when a certain coordinate is contributing photons, in our method the photon arrival time is spread out over the entire recording time of the image, which is longer by orders of magnitude. Although there are definite time points (i.e., commensurate with a multiple of the frame duration) at which the emission of one photon per molecule could happen at a certain coordinate, the detection event is so infrequent (probability << 1) that one does not know at which of these time points detection takes place. It could be the first or the last, or any of them in between. The setup can also be used in the slow scanning mode by using only galvanometer mirrors for both scan axes while the electro-optical deflector is passive.

The optical system was alternatively equipped with different laser sources and optical filters. A CW laser (VFL-P-1000-580, MPB Communications Inc.) operating at 580 nm was used as the STED source during the *Drosophila* experiments as indicated. Another CW setup employed a fiber laser (VFL-P-1000-592, MPB Communications Inc.) operating at 592 nm for STED and a pulsed super-continuum laser (SC450-4, Fianium Ltd.) with a repetition rate of 40 MHz for excitation. This laser was used mainly for samples labeled with yellow fluorescent protein. Various lines from 488 nm to 515 nm from the super-continuum source were selected with an acousto-optical tunable filter (97-02838-01, Crystal Technologies). The spatial overlay of the STED and excitation beams took place at a longpass filter (BLP01-561, Semrock Inc.), and the fluorescence signal was separated by a bandpass filter (FF01-559/34, Semrock Inc.). Here, the spatial shape of the STED beam was formed by a segmented wave plate[25] into a doughnut. For some measurements, a CW excitation source (2214-ML, JDS Uniphase Laser) at 488 nm and 515 nm was used. Additionally, an electro-optical modulator (LM0202, Linos Photonics GmbH) was placed in the optical path to block the illumination in predefined intervals during bleaching experiments. The system utilizes custom software implemented with LabView 8.5 (National Instruments). The code is available on request.

Figure 1b describes the scanning concept. A linear scan pattern is applied with the electro-optical scanner for the fast axis and with galvanometer mirrors for the slow axis. All images are scanned linearly backward and forward in both the (fast) x and (slow) y directions. The photons collected during the forward scan of a single line and during its backward counterpart are added and assigned to one line of one pixel height.

To calculate the number of pulses per diffraction-limited region by linear scanning, we use the following terms and formulas:

$$\text{excitation spot size:} \quad d = \frac{\lambda}{2 \times \mathrm{NA}}$$

$$\text{length of the fast scanned line:} \quad l_{\mathrm{fast}} = 2 \times f_{\mathrm{obj}} \times \varphi_{\mathrm{fast}}$$

$$\text{scan time per line for fast axis:} \quad t_{\mathrm{fast}}$$

with λ the wavelength of the focused light and NA the numerical aperture of the objective lens, f_{obj} the effective focal length of the objective lens and φ the deflection angle in the back focal plane.

From this, it follows that

$$\text{illumination time per spot}_{\mathrm{fast\_axis}} = t_{\mathrm{fast}} \times \frac{d}{l_{\mathrm{fast}}} = \frac{\lambda}{4 \times \mathrm{NA} \times f_{\mathrm{obj}}} \times \frac{t_{\mathrm{fast}}}{\varphi_{\mathrm{fast}}}$$

and that

$$\text{pulses per spot}_{\text{fast\_axis}} = \frac{\lambda}{4 \times \text{NA} \times f_{\text{obj}}} \times \frac{t_{\text{fast}}}{\varphi_{\text{fast}}} \times \text{laser repetition rate}$$

For the slow axis

$$\text{pulses per spot}_{\text{slow\_axis}} = \frac{\lambda}{4 \times \text{NA} \times f_{\text{obj}}} \times \frac{t_{\text{slow}}}{\varphi_{\text{slow}}} \times \frac{d}{l_{\text{fast}}} \times \text{laser repetition rate}$$

The third term in the product accounts for the pauses on a specific spot while the scanner addresses the same line but outside the specified spot. Hence, for 2D scanning

$$\text{pulses per spot}_{\text{2D}} = \frac{t_{\text{slow}} \times t_{\text{fast}}}{\varphi_{\text{slow}} \times \varphi_{\text{fast}}^2} \times \left(\frac{\lambda}{4 \times \text{NA} \times f_{\text{obj}}} \right)^3 \times \text{laser repetition rate}^2$$

Data filtering. Once single image frames are acquired by ultrafast scanning, different spatial and temporal filters can be applied to extract the vesicles and to track them beyond the diffraction limit. For example, the raw frames of **Figure 2a** were spatially filtered with a Gaussian of 100-nm width and temporally filtered over two frames. Filtered and raw video data are provided in **Supplementary Videos 3** and **4**. Note the true subdiffraction resolution, i.e., separation of objects at proximities/densities higher than that permitted in single-particle tracking techniques for (by definition) isolated objects.

Sample preparation. *Fixed HIV.* HIV (EGFP fused to the accessory protein Vpr, provided by J.C.) were prepared on fibronectin-coated cover slips. They were fixed with paraformaldehyde and embedded in Mowiol/DAPCO.

TAT-EGFP samples. TAT-EGFP (genetic fusion of the TAT cell-penetrating peptide sequence GRKKRRQRRRPQ and EGFP) was purified from BL21 cells via a GST tag that was enzymatically cleaved after purification. CV-1 (monkey epithelial kidney) cells, grown on #1.5 glass coverslips were incubated with 4 µM TAT-EGFP in PBS for 10 min at 37 °C, allowing for endosomal internalization. Cells were then washed three times with PBS and fixed using 3% paraformaldehyde. Finally, fixed cells were mounted in Mowiol (Sigma-Aldrich, Munich) and imaged as described. These samples were kindly provided by D. Richardson and C. Gregor.

DNA single strands. To obtain ssDNA samples, we stained λ DNA with YOYO (Invitrogen) in a ratio of 1:5 and combed the DNA on glass substrates. The single strands were imaged in ROXS buffer (pH 8.0)[26].

Fixed fluorescent beads. Coverslips were cleaned thoroughly with ethanol in an ultrasonic bath, immersed in 200 µl poly(L-lysine) for 10 min (Sigma-Aldrich) and rinsed with distilled water. Yellow-green fluorescent beads (Invitrogen) were diluted 1: 100,000 in distilled water. The coverslips were then incubated for 10 min with the suspension and rinsed with distilled water. They were sealed using nail polish and a second coverslip with 20 µl Mowiol (with DAPCO) as immersion medium between them.

Immunofluorescence staining for fluorescence yield experiments. To obtain a stable and dense staining of microtubules, REF cells were fixed in 4% paraformaldehyde before incubating with the primary antibody. After washing with PBS, the second antibody with Atto 465/Alexa 488/Oregon Green label was incubated. After intense washing, the samples were imbedded in Mowiol with DAPCO.

Single antibodies. Samples of disperse, single anti-rabbit IgG–Atto 647N antibodies produced in goat (Sigma) were created by cleaning standard cover glasses for 10 min in 2% Mucasol solution in an ultrasonic bath, coating them with poly(L-lysine) solution for 10 min and letting antibodies from a diluted solution (1:30,000 in PBS) attach to the surface for 10 min. Slides were embedded in Mowiol with Trolox on microscope object slides, which had been cleaned as described above and irradiated with UV light for 10 min (for Trolox activation) directly before imaging.

Diffusing fluorescent beads. Yellow-green fluorescent beads (100 nm, Invitrogen), distilled water and glycerol were mixed in a ratio of 1:100:100. Coverslips and glass slides were precleaned thoroughly with ethanol in an ultrasonic bath. The suspension was pressed between a coverslip and a glass slide such that the majority of beads was diffusing and a few got attached to the coverslip.

Drosophila *samples.* Third instar larvae were selected, rinsed with water and dab dried before being placed on a thin layer of halocarbon oil in a custom-built imaging chamber. To anesthetize the larvae, we applied 90 µl 100% (v/v) Forene (Abbott) to the imaging chamber. After 5 min the *in vivo* imaging was performed.

Dynamic HIV. VSV-G–pseudotyped HIV-1 particles were prepared from the tissue culture supernatant of 293T cells cotransfected using polyethylenimine (PEI) with 7 µg of pCHIV Env(−), 7 µg of pCHIV MA.EGFP Env(−), 1 µg of pEGFP.Vpr (a kind gift from T. Hope) and 2.5 µg of VSV-G protein expression plasmid. Tissue culture supernatants were harvested 48 h after transfection or infection and cleared by filtration through a 0.45-mm nitrocellulose filter. Particles were then purified by centrifugation through a 20% (w/w) sucrose cushion at 70,000*g* for 2 h at 4 °C. Pelleted particles were resuspended in ice-cold 20 mM HEPES/PBS, pH 7.4, frozen rapidly in liquid nitrogen and stored in aliquots at −80 °C. Virus particles were adhered to HeLa EMBL cells for 2 h at 16 °C. Excess particles were removed by a medium exchange with Opti-MEM (Invitrogen). Samples were transferred to the 37 °C–heated microscope stage and imaged live in both confocal and STED modes.

The authenticity of the certified cell lines used was documented by the providers. The mycoplasma-free state of cell lines was regularly assessed in line with good laboratory practice. No biological conclusions are drawn in this work.

Code availability. The custom software is freely available. Please contact the corresponding author.

24. Bingen, P., Reuss, M., Engelhardt, J. & Hell, S.W. *Opt. Express* **19**, 23716–23726 (2011).
25. Reuss, M., Engelhardt, J. & Hell, S.W. *Opt. Express* **18**, 1049–1058 (2010).
26. Vogelsang, J. *et al. Angew. Chem. Int. Ed.* **47**, 5465–5469 (2008).

doi:10.1038/nmeth.3481